Metallurgical and Materials Engineering *Scientific paper*
Association of Metallurgical Engineers of Serbia AMES *https://doi.org/10.30544/398*

BISPHENOL A REMOVAL FROM AQUEOUS SOLUTION USING FINE α-Fe_2O_3 PARTICLES

Nataša Z. Tomić[*1], *Marija M. Vuksanović*[1], *Đorđe N. Veljović*[2], *Aleksandar D. Marinković*[2], *Vesna J. Radojević*[2], *Radmila M. Jančić Heinemann*[2]

[1]*Innovation Center of Faculty of Technology and Metallurgy, Karnegijeva 4, 11070 Belgrade, Serbia*
[2]*University of Belgrade, Faculty of Technology and Metallurgy, Karnegijeva 4, 11070 Belgrade, Serbia*

Received 23.10.2018.
Accepted 11.12.2018.

Abstract

Iron(III) oxide particles (α-Fe_2O_3) were obtained from ferrous chloride ($FeCl_3 \cdot 6H_2O$) precursor using ammonium hydroxide as a precipitating agent and particles were calcined at 700 °C for 4 h. Morphological and structural properties of the obtained particles were determined using Scanning Electron Microscopy (SEM), BET/BJH analysis, X-ray diffraction (XRD) and Fourier Transform Infra-Red (FT-IR). The image analysis software, Image-Pro Plus 4.0, was used to determine the distribution of the diameter of the obtained particles. Hematite based particles were used as an adsorbent for BPA removal. Adsorption equilibrium was established after 75 min with 14.8% BPA removal efficiency.

Keywords: Bisphenol A; adsorption; α-Fe_2O_3; precipitation method.

Introduction

Iron(III) oxide (Fe_2O_3) has four crystallographic phases, explicitly hematite (α-Fe_2O_3), β-Fe_2O_3, maghemite (γ-Fe_2O_3) and ε-Fe_2O_3 [1], which represents one of the main focuses of modern material science. The most stable iron oxide, α-Fe_2O_3, is widespread and it is found in aquatic systems, lands, and sediments. Hematite has diverse applications in catalysis, pigments, biomedical materials, lithium batteries, electromagnetic devices, adsorbents [2,3]. The synthesis of hematite particles has increased in recent decades due to its unique electrical, optical and magnetic properties [4,5]. There are different techniques for the synthesis of hematite, and one of them is the co-precipitation method [6].

* Corresponding author: Nataša Z. Tomić, *ntomic@tmf.bg.ac.rs*

Bisphenol A (BPA) is widely used in the production of polycarbonates, epoxy resins, plasticizers, retardants [7], dental materials, dental gaskets, food linings, and drinking containers, as well as many other products [8]. The main problem of BPA lies in its physical-chemical properties such as low solubility and high hydrophobicity, which lead to its low biodegradability and accumulate in living organisms [9]. BPA at low concentrations can cause infertility and breast cancer, so wastewater containing BPA must be adequately treated before discharge into the environment [10] Therefore, the development of a fast and effective method for removing BPA is of great importance. Today, among many techniques in wastewater treatment, adsorption, with relatively high capacity and low cost, is the most widely used [11]. Various nanomaterials such as magnetite nanoparticle can be used as adsorbents for the removal of toxic pollutants [12]. Literature shows the use of various conventional and non-conventional adsorbents for BPA removal from water. It is evident that the modified adsorbents and composite materials show promising results for BPA removal from water [13].

This paper aims to synthesize α-Fe_2O_3 particles by precipitation method for Bisphenol A removal.

Experimental procedure

Materials

Iron(III) chloride ($FeCl_3 \cdot 6\ H_2O$) was purchased in the crystallized state from the Clariant company. Sigma Aldrich supplied ammonium hydroxide (NH4OH) and Bisphenol A. Deionized water was used in all experiments.

Preparation of fine α-Fe_2O_3 particles

Pure α-Fe_2O_3 particles were synthesized by chemical precipitation method [14]. According to this procedure, the aqueous solution was prepared by dissolving 5 g of iron(III) chloride hexahydrate ($FeCl_3 \cdot 6H_2O$) in 100 mL of deoxygenated distilled water under magnetic stirring for 30 min 50 mL of 2M aqueous solution of NH_4OH, used as the precipitating agent, was gradually added dropwise to maintain a pH value of 11. The resulting precipitations were collected and centrifuged at 6000 rpm and then washed with distilled water and ethanol several times and finally dried in air. The produced powder was calcined at 700 °C for 4 h in order to obtain α-Fe_2O_3 particles.

Characterization methods

The morphology of α-Fe_2O_3 particles was examined using the FESEM, MIRA 3 TESCAN electron microscope operated at 20 kV. The image analysis tool (Image-Pro Plus 4.0, Media Cybernetics) was used to obtain the particles diameter distribution.

Textural properties of α-Fe_2O_3 particles (specific surface area and porosity characteristics) were determined by the Brunauer-Emmett-Teller (BET) method using a Micromeritics ASAP2020 surface area and porosity analyzer.

X-ray diffraction (XRD) patterns were recorded on an Ital Structure APD2000 X-ray diffractometer in a Bragg–Brentano geometry using CuKα radiation (λ = 1.5418 Å) and step-scan mode (range: 20−90° 2θ, step-time: 0.5 s, step-width: 0.02°). The PowderCell program [W. Kraus, G. Nolze, PowderCell for Windows, V.2.4, Federal Institute for Materials Research and Testing, Berlin, Germany, 2000.] was used for approximate phase analysis.

The structural analysis of calcined particles was performed by single-beam Fourier-Transfer Infrared Spectroscopy (FTIR) using a Nicolet iS10 spectrometer (Thermo Scientific) in the attenuated total reflectance (ATR) mode with a single bounce 45 °F Golden Gate ATR accessory with a diamond crystal, and DTGS detector. FTIR spectra were obtained at 4 cm^{-1} resolution with ATR correction. The FTIR spectrometer was equipped with OMNIC software and the spectra were recorded in the wavelength range from 2.5 μm to 20 μm (i.e., 4000 –500 cm^{-1}).

The concentrations of the bisphenol A were determined using UV-Vis spectroscopy (Shimadzu UV-1800 spectrophotometer).

A laboratory pH meter, InoLab Cond 730 precision conductivity meter (WTW GmbH), with an accuracy of ± 0.01 pH units, was used for the pH measurements. The pH values at the point of zero charges (pH_{PZC}) were measured using the pH drift method, before and after BPA adsorption [15].

Adsorption measurements

Batch adsorption experiments of BPA were applied in order to evaluate the performance of the α-Fe_2O_3 adsorbents. A suspension of the adsorbent material (m/V= 200 mg/L), was mixed on a magnetic stirrer containing an aqueous solution of BPA (C_0 = 20 mg/L) at pH 6. The mixture was stirred in the dark for 75 min to reach adsorption equilibrium. The concentration of BPA was measured by withdrawing quantitative aliquots (1.0 ml) from the mixture at regular time intervals according to the peak at 276 nm by UV-Vis spectroscopy.

The mean value from three determinations was used for processing the experimental data. The percentage of adsorbed BPA was calculated using Equation (1):

$$Removal\ efficiency\ (\%) = \left(\frac{C_i - C_f}{C_i}\right) \cdot 100\% \qquad (1)$$

where C_i and C_f are the initial equilibrium and final concentrations of BPA in the solution in mg/L, respectively. The adsorption capacity of BPA was determined according to the mass balance equation, Equation (2):

$$q_e = \left(\frac{C_i - C_f}{m}\right) \cdot V \qquad (2)$$

where q_e is the adsorption capacity in mg/g adsorbent, V is the volume of solution in L, and m is the mass of the adsorbent in g.

Results and discussion

The microstructure of α-Fe2O3 particles

The SEM micrograph of α-Fe_2O_3 particles and their mean diameter (D_{mean}, nm) distribution are shown in Figure 1. Determined textural characteristics are presented in Table 1.

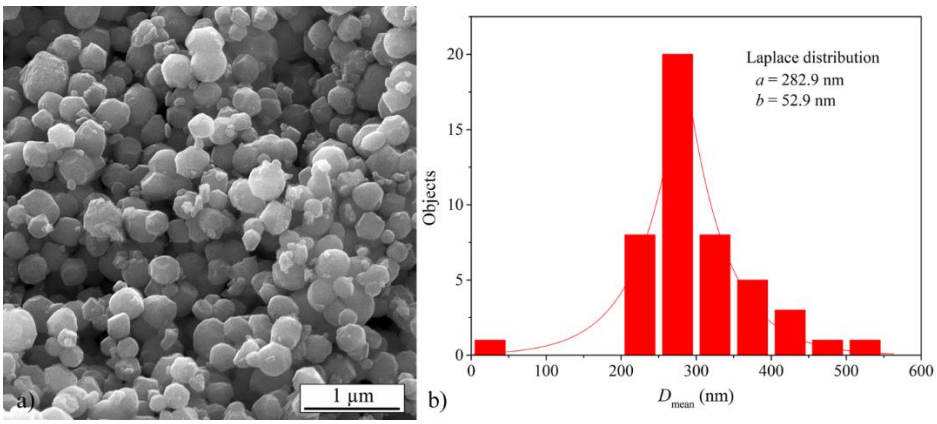

Fig. 1. α-Fe_2O_3 particles: a) SEM microphotograph, and b) mean diameter distribution.

Table 1. Textural characteristics of α-Fe_2O_3 particles.

Parameter/Sample	α-Fe_2O_3
Specific surface area, S_{BET} (m^2/g)	2.788
Total pore volume, V_{total} (cm^3/g)	0.009
Mesopore volume, V_{meso} (cm^3/g)	0.009
Mean mesopore diameter, D_{mean} (nm)	13.708
pH_{PZC}	5.1

Figure 1a shows the spherical shape of particles whose diameter distribution is fairly uniform. The mean diameter distribution is best described by Laplace distribution with the location parameter a = 282.9 nm and scale parameter b = 52.9 nm, Figure 1b. The location parameter indicates the value of D_{mean} with the highest probability. The scale parameter shows the size of a distribution spreading which is up to 18.7%. The range of distribution is between 25.67 – 523.19 nm. Obtained results indicate the size of the particles that correspond to the ˋfine particles′ with a fraction in nanodomain. Textural characteristics of α-Fe_2O_3 suggest low porosity of particles when compared to most of the adsorbents used for BPA removal [13]. A mesoporosity can provide good adsorption of BPA to the surface of α-Fe_2O_3.

The structural characterization of particles

The composition of Fe_2O_3 observed by X-ray diffraction (XRD) for identifying the crystalline structure, and Fourier Transform Infra-Red (FTIR) spectroscopy, is presented in Figure 2.

Obtained XRD diffractogram, Figure 2a, was analyzed and the sample was identified as a stable α-Fe_2O_3 (hematite) form (ICSD 161294 card). The mean crystallite size of α-Fe_2O_3 phase was estimated from the most intense diffraction peaks by the PowderCell software. The unit cell parameters of α-Fe_2O_3 are a = 5.0282 and c = 13.7250 Å. The mean crystallite size of α-Fe_2O_3 phase is 34.4 nm, Figure 2a.

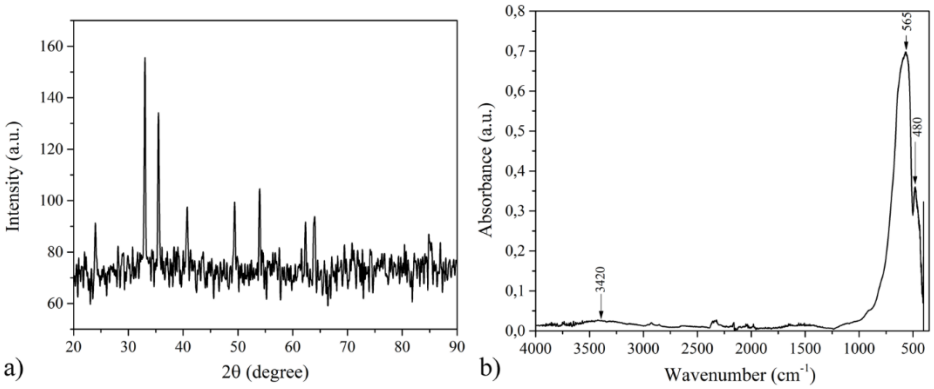

Fig. 2. a) XRD patterns of α-Fe_2O_3 phase and b) Spectra FTIR of α-Fe_2O_3 particles synthesized by precipitation method.

XRD diffractogram shows clear and intense peaks corresponding to a rhombohedral crystalline structure of the well-crystallized α-Fe_2O_3 sample. The FTIR spectrum (Figure 2b) shows the absorption at 3420 cm^{-1} that is assigned to stretching vibrations of hydroxyl groups [16]. The sharp absorption peaks at 480 and 565 cm^{-1} can be attributed to the Fe–O band vibrations of the calcined hematite synthesized by the precipitation method, Figure 2b [17,18].

Adsorption study

The removal efficiency, followed by UV-Vis spectroscopy, versus adsorption time is presented in Figure 3. The highest increase in removal efficiency is noticed between 25 and 30 min of adsorption. Adsorption equilibrium is established after 75 min with 14.8% removal efficiency. α- Fe_2O_3 particles used as adsorbent showed adsorption capacity at equilibrium for BPA removal q_e = 14.8 mg/g.

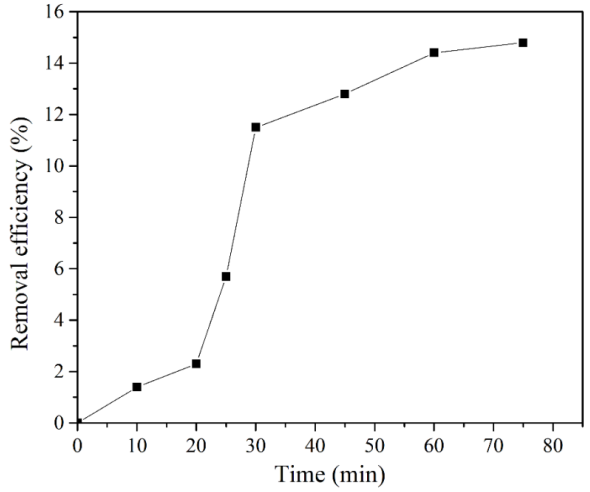

Fig. 3 The efficiency of BPA removal versus adsorption time.

Comparison of adsorption performance of α-Fe_2O_3 particles was difficult to perform due to the insufficient literature data for application of hematite for BPA removal in adsorption experiments. Available data for adsorption capacities of adsorbents used for BPA removal were summarized in Table 2. The adsorption capacity of α-Fe_2O_3 particles at low dosage may indicate competitive adsorption properties suggesting the potential use of α-Fe_2O_3 particles as an economic and effective mineral adsorbent for BPA removal.

Table 2. Comparative results of different adsorption studies for BPA removal.

Adsorbent	Dosage	Capacity	Ref.
Fe(III)/Cr(III) hydroxide-untreated	10000 mg/L	3.47 mg/g	[19]
Fe(III)/Cr(III) hydroxide-pretreated	10000 mg/L	3.67 mg/g	[18]
P-phenylenediamine-modified magnetic graphene oxide	250 mg/L	155.0 mg/g	[20]
Iron-oxide/activated carbon (PAC) (Hematite/PAC, Magnetite/ PAC, Ferrihydrite/PAC)	1000 mg/L	~0.60 mg/g	[21]
Goethite/PAC	167 mg/L	1.00 mg/g	[22]
Goethite	167 mg/L	1.00 mg/g	[21]
Fe_3O_4@polyaniline core-shell nanoparticles	3200 mg/L	9.13 mg/g	[23]
α-Fe_2O_3	200 mg/L	14.8 mg/g	this paper

Conclusions

The iron(III) oxide particles were prepared by a co-precipitation method and calcination at 700 °C. The obtained particles were identified as a stable α-Fe_2O_3 (hematite) phase by X-ray diffraction. In addition to the variety of investigated adsorbents in literature, there is a lack of knowledge of the adsorption properties of α-Fe_2O_3 particles for BPA removal. This study aimed to examine the effects of BPA removal from aqueous solution by α-Fe_2O_3 nanoparticles. Particle size was characterized by image analysis of SEM micrographs. Mean diameter was best described by its median value – 282.9 nm. Textural characteristics of α-Fe_2O_3 showed low porosity of particles having a specific surface area – 2.788 m^2/g. Furthermore, adsorption capacity at equilibrium for BPA removal was q_e = 14.8 mg/g which may indicate competitive use of α-Fe_2O_3 particles as an economical and effective mineral adsorbent for BPA removal.

Acknowledgments

This research has been financed by the Ministry of Education, Science and Technological Development of the Republic of Serbia as a part of the project TR34011.

References

[1] S. Sakurai, A. Namai, K. Hashimoto, S.I. Ohkoshi: Am Chem Soc, 131 (2009) 18299–18303.
[2] J. Shakhpure, H. Vijayanand, S. Basavaraja, V. Hiremath, A. Venkatraman: Bull Mater Sci, 28 (2005) 713–718.
[3] M. Zhu, Y. Wang, D. Meng, X. Qin, G. Diao: Phys Chem C, 116 (2012) 16276–1628.
[4] A.P. Alivisatos: Sci New Ser, 271 (1996) 933–937.

[5] V.L. Colvin, M.C. Schlamp, A.P. Alivisatos: Nature, 370 (1994) 354–357.
[6] A. Lassoued, M.S. Lassoued, B. Dkhil, S. Ammar, A. Gadri: Phys E Low-dimens Syst Nanostruct, 101 (2018) 212–219.
[7] J. Xu, L. Wang, Y. F. Zhu: Langmuir, 28 (2012) 8418–8425.
[8] B.S. Rubin: J Steroid Biochem Mol Biol, 127 (2011) 27–34.
[9] J. Bohdziewicz, G. Liszczyk: Ecol Chem Eng S, 20 (2013) 371–379.
[10] C.S. Guo, M. Ge, L. Liu, G.D. Gao, Y.C. Feng, Y.Q. Wang: Sci Technol, 44 (2010) 419–425.
[11] G. Bayramoglu, M.Y. Arica, G. Liman, O. Celikbicak, B. Salih: Chemosphere, 150 (2016) 275–284.
[12] T. Safabakhsh, H. Pourzamani: Int J Env Health Eng, 5 (2016) 25.
[13] A. Bhatnagar, I. Anastopoulos: Chemosphere, 168 (2017) 885-902.
[14] A. Lassoued, M. S. Lassoued, B. Dkhil, S. Ammar, A. Gadri: Physica E Low Dimens Syst Nanostruct, 101 (2018) 212–219.
[15] D. Budimirović, Z. S. Veličković, V. R. Djokić, M. Milosavljević, J. Markovski, S. Lević, A.D. Marinković: Chem Eng Res Des, 119 (2017) 75.
[16] Y. Xu, H. Bai, G. Lu, C. Li, G. Shi: J Am Chem Soc, 130 (2008) 5856–5857.
[17] H. Liu, P. Li, B. Lu, Y. Wei, Y. Sun: Solid State Chem, 182 (2009) 1767–1771.
[18] A. Lassoued, M.S. Lassoued, B. Dkhil, A. Gadri, S. Ammar: J Mol Struct, 1148 (2017) 276–281.
[19] C. Namasivayam, S. Sumithra: Clean Technol Environ Policy, 9 (2007) 215–223.
[20] X. Tang, P. Tang, S. Si, L. Liu: J Serb Chem Soc, 82 (2017) 39–50.
[21] H. S. Park, J. R. Koduru, K.-H. Choo, B. Lee: J Hazard Mater, 286 (2015) 315–324.
[22] J. R. Koduru, L. P. Lingamdinne, J. Singh, K.-H. Choo: Process Saf Environ, 103 (2016) 87–96.
[23] Q. Zhou, Y. Wang, J. Xiao, H. Fan: Synth Met, 212 (2016) 113–122.